

# PADLOC: Physically-Aware Defect Localization and Characterization

Soumya Mittal and R. D. (Shawn) Blanton  
Advanced Chip Test Laboratory  
Department of Electrical and Computer Engineering  
Carnegie Mellon University  
Pittsburgh, USA  
<http://www.ece.cmu.edu/~actl/>  
{soumyami, blanton}@ece.cmu.edu

**Abstract**—Software-based diagnosis examines the failing-circuit design and test response to identify potential defect locations and if possible, pinpoint the root cause of failure. This paper describes a generalized physically-aware methodology called PADLOC (Physically-Aware Defect Localization and Characterization) to improve the quality of diagnosis. PADLOC consists of (a) identifying the subnets that are more likely to correspond to the actual defect, and (b) deriving the defect behavior based on the activity of the neighborhood (i.e., nets that are physically close and logically related). Results from 6,000 defect injection experiments reveal that 97.2% of the defects are accurately diagnosed with 92.6% of defects achieving a logical resolution of at most five and 27.6% of defects attaining perfect resolution. PADLOC has an average resolution of 2.6 and improves resolution for 24.8% of defects over prior work. In addition, the physical resolution (i.e., number of subnets) is improved for 61.3% of defects. Finally, PADLOC returns 33.9 fewer subnets per defect and reduces the number of subnets by 44.8%.

**Keywords**—diagnosis; testing; defect; layout; cell; open; bridge

## I. INTRODUCTION

Physical failure analysis (PFA) is the process of identifying the root cause of failure within an integrated circuit (IC) by visually examining the IC for defects. The information obtained from PFA is used to understand failure mechanisms and to correct the manufacturing process and/or the design to eliminate defects in order to improve yield and reliability. This process however is often destructive, time-consuming and not always successful, and is thus applied to only a small number of ICs. To improve the likelihood of failure analysis success, PFA is usually preceded by diagnosis. Diagnosis is a software-based process of determining the possible locations (often called candidates) and the corresponding defect types within a failing IC. The defect locations identified by diagnosis can then be visually inspected for PFA. The quality of diagnosis is typically measured by the number of candidates found (known as diagnostic resolution) and whether the candidate set contains an actual defect location (typically referred to as diagnosis accuracy), and critically impacts the success rate of PFA. Another important measure of diagnosis is the capability to characterize the failure that includes (a) identifying the defect type, (b) the precise  $x$ - $y$ - $z$  layout

location of the defect, and (c) deriving its precise impact on circuit behavior, which is accomplished here through the derivation of a customized fault model.

Determining the location of a defect is the typical objective of diagnosis. Ideally, diagnosis should go beyond localization to characterizing both the nature and root cause of a defect. Besides supplementing PFA, diagnoses outcomes of a large number of ICs can be used to achieve other goals. For example, diagnoses results can be correlated to discover if a substantial percentage are failing due to a common root cause [1]. It has also been shown that information obtained from diagnoses can be used to estimate defect density and size distribution [2], and defect-type distribution [3]. Work in [4] uses diagnoses data to learn the effectiveness of different fault models and test metrics without performing conventional test-set silicon experiments. In [5], diagnosis is used to predict IC defect level and monitor IC quality. Because diagnosis is becoming useful for other applications, and PFA is becoming more challenging with advancing technology, it is imperative that diagnosis continue to improve and move toward characterization.

Several papers have been published over the years that improve the diagnosability of a failed IC. Algorithms such as the ones described in [6]–[10] utilize a logic-level description of the design to find a possible cause and location of the failure. These approaches compare the observed circuit response with predetermined faulty behaviors at the logic level to obtain logical locations, analyze the defective behavior and identify locations that could have caused the observed failures, or use a combination thereof to enhance the quality of diagnosis.

However, these approaches, in general, cannot pinpoint the physical location of the defect. Thus, approaches such as [11]–[24] incorporate design layout information in the diagnosis flow to improve the resolution and accuracy of diagnosis. For example, diagnosis techniques of [11]–[16] are centered only on open defects, while the technique presented in [17] focuses on bridge defects. These “defect-based” diagnosis approaches are distinguished from the ones described in [18]–[24] by the fact that they focus on a specific defect type. Methods presented in [18]–[21] are

applicable to different defect types but do not focus on deriving defect behaviors.

The unpredictability of defects requires the use of a more generalized approach to defect diagnosis, or a multitude of defect-based approaches. But the disadvantage of using a set of defect-based approaches is the possibility that some defect behavior is missed. One general approach, referred to as DIAGNOSIX, is described in [22]–[24]. It is one of the first physically-aware diagnosis methods that is applicable to any defect type and handles defects exhibiting arbitrary characteristics as well. Instead of correlating observed defect behavior with fault models to locate defects, it derives the defect behavior by analyzing the logic activity of the nets surrounding its location.

This work describes a diagnosis methodology that we term PADLOC (Physically-Aware Defect Localization and Characterization) which builds on DIAGNOSIX but with several improvements. Specifically, PADLOC has the following features:

- Enhanced defect localization using minimal layout information.
- Defect behavior is derived based on its neighborhood, instead of relying on specific fault models.
- It is applicable to localized defects that exhibit a variety of misbehaviors.

The rest of the paper is organized as follows. A brief background on DIAGNOSIX is described in Section II. Section III describes an approach to improve defect localization by dividing a net into segments and identifying their neighborhood. Experiment results are presented in Section IV. The final section concludes the paper.

## II. BACKGROUND

DIAGNOSIX [22]–[24] is a comprehensive physically-aware diagnosis approach that finds potential defect locations without using a particular fault model, and derives a customized fault model that represents the defect behavior at each location. In that work, a candidate is assumed to be controlled by the nets surrounding its location. This observation is quite conservative and holds true for a variety of defects that includes bridge, open, and cell defects. The nets near the candidate are collectively referred to as its neighborhood, and includes all nets that are in physical proximity to the candidate, the inputs of the cell driving the candidate, and the side-inputs of the cells being driven by the candidate. The logic values established in the neighborhood of a candidate form its neighborhood state. The neighborhood state can also be dynamic in nature for sequence- and timing-dependent defects. Thus, in DIAGNOSIX, the excitation of a defect at candidate location is assumed to be a function of its neighborhood state.

Design layout is analyzed to find the physical neighbors of a net. Specifically, every neighboring net within some carefully-chosen distance  $d$  of the candidate is considered

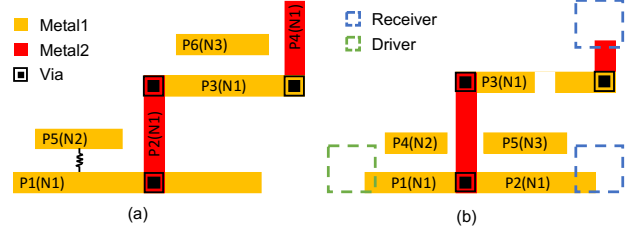


Fig. 1. Example showing how all neighbors of a net, as identified from DIAGNOSIX, are not relevant to excite (a) a bridge and (b) an open defect.

a physical neighbor of that candidate. Note that only intra-layer proximity is used to identify physical neighbors in that work.

Neighborhood states for each candidate are collected for Tester-Fail-Simulation-Fail (TFSF) and Tester-Pass-Simulation-Fail (TPSF) patterns. Here, a TFSF (TPSF) is a pattern that fails (passes) on the tester and detects either of the stuck-at faults at the candidate location. For a candidate to be considered as consistent, the sets of neighborhood states for TPSF and TFSF patterns should be disjoint. In other words, if the neighborhood state of a candidate is the same for any pair of TFSF and TPSF patterns, then the candidate has demonstrated inconsistency. In DIAGNOSIX, a candidate is eliminated from further consideration based on inconsistency. Consistency has been shown to be an effective method for improving resolution in [22]–[25].

DIAGNOSIX can be improved in several ways. First, the candidates reported by DIAGNOSIX are logical signals. However, the net that corresponds to the logical signal can be long and can span various metal layers. Examining a long net increases PFA effort. Thus, it is beneficial to improve the physical resolution [26] by identifying a net segment that is more likely to correspond to the actual defect location.

Second, not all neighbors of a net are relevant to defect excitation. Fig. 1(a) illustrates this point for a bridge defect. Each segment in Fig. 1(a) is assigned a name, and is denoted by ‘segment name(net name)’. As shown,  $P5(N2)$  and  $P6(N3)$  are physical neighbors of  $P1(N1)$  and  $P3(N1)$ , respectively. Consider a bridge defect (shown as a resistor) involving segments  $P1(N1)$  and  $P5(N2)$ . DIAGNOSIX assumes that neighbor  $P6(N3)$  can influence the faulty value of  $N1$ , irrespective of the defect location. However, the logic value of  $P6(N3)$  is less likely to influence the value at the bridged subnets because  $P6(N3)$  is not physically close to the defect location. Net  $N3$  can affect the faulty value of  $N1$  only when there is a bridge defect involving  $P3(N1)$ . Thus, identifying relevant neighbors of a defect location can improve the physical resolution.

Similarly, Fig. 1(b) illustrates this observation for an open defect. Consider an open defect located at  $P3(N1)$ , depicted as missing metal material. DIAGNOSIX assumes that the physical neighbors of  $N1$  will control the value of the open net. However, the value at the floating net can only

be influenced by the physical neighbors downstream<sup>1</sup> from the defect location. Thus, contrary to the assumption by DIAGNOSIX,  $N1$  neighbors,  $P4(N2)$  and  $P5(N3)$ , are unlikely to play a role in deciding the value at the floating segment.

The first limitation can be addressed by partitioning a net into segments. Each segment would have its own set of neighbors. The partitioning would not only decrease the size of neighborhood, but also improve the physical resolution. The criterion used for dividing each net into segments depends on the surrounding circuitry and is explained in Section III. The choice of criterion would address the second shortcoming associated with DIAGNOSIX.

### III. NEIGHBORHOOD IDENTIFICATION

Various techniques have been proposed in the literature that improve the diagnosis of open and bridge defects using layout information. Techniques such as [18] extract features prone to bridge defects from layout using Design Rule Check (DRC) and Design for Manufacturability (DFM) guidelines. Potential bridge locations can also be derived using proximity analysis where a net can form a bridge with any net that is adjacent to it [21]–[24]. Another approach is to find pairs of nets that are capacitively coupled via circuit parasitics. Using DFM guidelines and extracting accurate capacitances may not be feasible, especially for advanced nanometer technologies. Specifically, as technology advances, increases in design size and circuit density results in an increase in the number of parasitics and more importantly their complexity, which significantly impacts the performance of an electromagnetic field solver required to obtain accurate parasitics.

As mentioned earlier, tracing a candidate net during PFA can be an expensive task depending on several factors including its length and number of metal layers it resides in. To improve localization, each single via in the design is considered as a potential defect location in [18]. In [19], in addition to via-related features such as single, multiple, stacked and stress vias, minimum width nets with nets on either side at minimum spacing are also considered prone to open defects.

A “segment” model is presented in [11], [21], where each net is partitioned into segments such that each segment drives a different set of receiver cells. Partitioning in this way improves localization because only smaller parts of a net require examination instead of the entire net.

In [12], a via that is more prone to be defective is identified using the parasitic capacitance that exists between the corresponding floating net segment and its adjacent nets, and the trapped charge on the floating segment. The technique of [13] improves upon [12] by taking into account the internal capacitances and the logic threshold voltages

of the receiver cell(s). In addition to using these circuit parameters, the technique of [14] also analyzes the effect of process variations on the voltage of the floating net. However, as reasoned earlier, methods that rely on these parameters are not desirable as their values may not be accurately known at advanced nodes.

An approach to locate open vias without the use of low-level (and possibly inaccurate) parameters is presented in [15]. For each net segment driving  $N$  cells,  $2^N - 1$  combinations of multiple faults are simulated to identify the fault combinations (i.e., segments as identified using [11]) whose response match the observed circuit response. For a segment with a large fan-out, performing fault simulation for all  $2^N - 1$  multiple faults would be impractical.

Another similar approach, described in [16], is based on the idea that the logic value at the candidate is a weighted majority function of the logic values at the neighbors, where neighbors closer to the candidate are more influential. This method has a similar drawback to one within DIAGNOSIX, that is, the voltage at the floating net is unlikely to be influenced by the neighbors upstream from the defect location (Fig. 1(b)).

In this work, to improve localization of bridge defects, each net is divided into segments where (a) each segment has its own set of physical neighbors and (b) a segment and its physical neighbors reside in the same metal layer<sup>2</sup>. This is illustrated in Fig. 2. Each segment in Fig. 2 is assigned a name, and is denoted by ‘segment name(net name)’. Net  $N1$  is partitioned into five segments  $\{P1, P2, P3, P4, P5\}$ . The physical neighborhood of each segment of  $N1$  is given in Table 1.

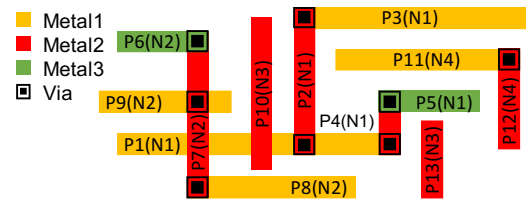


Fig. 2. Illustration of net partitioning into segments for localizing bridge defects.

TABLE 1  
PHYSICAL NEIGHBORHOOD FOR EACH SEGMENT OF NET  $N1$  (FIG. 2)  
FOR BRIDGE DEFECT DIAGNOSIS.

Segment	Physical neighborhood
$P1$	$P8, P9$
$P2$	$P10$
$P3$	$P11$
$P4$	$P13$
$P5$	-

To improve the diagnosis of open defects, each net is partitioned into segments where (a) each segment drives

<sup>1</sup>Downstream (upstream) is the net segment between the receiver cells (driver cell) and the open-defect location.

<sup>2</sup>Although intra-layer proximity is used in current analyses and experiments, inter-layer neighborhood identification can also easily be accomplished.

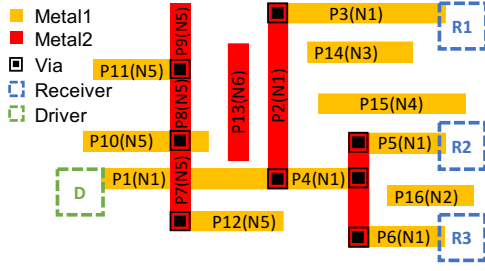


Fig. 3. Illustration of net partitioning into segments for localizing open defects.

a unique set of receiver cells and (b) each segment has a unique physical neighborhood. The physical neighborhood of each segment comprises of all the physical neighbors of the downstream segments and the segment itself. This occurs because voltage at the floating node is not only influenced by the nets adjacent to it, but also (possibly) by the nets in the vicinity of the downstream segments.

Segment partitioning for open defect diagnosis is illustrated in Fig. 3. The cell driving and the cells being driven by net  $N1$  are represented with dashed green and blue squares, respectively. Using this approach,  $N1$  would be divided into six segments -  $P1$  driving the cells  $\{R1, R2, R3\}$ ,  $P2$  and  $P3$  driving  $\{R1\}$ ,  $P4$  driving  $\{R2, R3\}$ ,  $P5$  driving  $\{R2\}$ , and  $P6$  driving  $\{R3\}$ .

The physical neighborhood of each segment of  $N1$  is shown in Table 2. The method of [11] would consider  $P2$  and  $P3$  as one segment because both affect the same set of receivers. Here, they are considered as two segments because of the difference in their physical neighbors;  $P13$  is a neighbor of a segment upstream from  $P3$  and thus is unlikely to affect its logic value.

TABLE 2  
PHYSICAL NEIGHBORHOOD FOR EACH SEGMENT OF NET  $N1$  (FIG. 3)  
FOR OPEN DEFECT DIAGNOSIS.

Segment	Physical neighborhood
$P1$	$P10, P12, P13, P14, P15, P16$
$P2$	$P13, P14$
$P3$	$P14$
$P4$	$P15, P16$
$P5$	$P15$
$P6$	$P16$

Recall that there are two components of a neighborhood of a net - physical and logical. In DIAGNOSIX, the logical neighbors of a net consists of the inputs of the cell driving the net and the side-inputs of the cells being driven by the net. However, the logical neighbors play different roles for different defect types. For example, the voltage of bridged nets depends on the logic values of the inputs of the cells driving these nets and the state of the surrounding circuit [27].

An example circuit shown in Fig. 4 illustrates the process of identifying logical neighbors that are more likely to be involved with an open defect. Suppose that the topology of

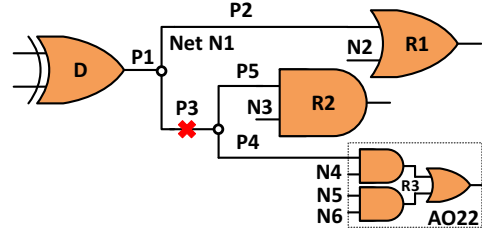


Fig. 4. An example defective circuit illustrating the identification of relevant logical neighbors.

net  $N1$  in the layout of the circuit is similar to that shown in the schematic in Fig. 4. Further suppose that the net partitioning for open defect diagnosis results in five segments,  $P1 - P5$ . For an open defect (strong open) at segment  $P3$  (net  $N1$ ), two observations are made. First, the inputs of cell  $D$  cannot influence the logic value at the floating part of  $P3$  because the output of  $D$  is disconnected from it. Second, as  $P3$  drives the cells,  $R2$  and  $R3$ , only side-inputs of these two cells would form its logical neighborhood. Thus, in this case, the logical neighborhood consists of the nets  $\{N3, N4, N5, N6\}$ .

Furthermore, each side-input of a basic cell such as AND, NAND, OR, NOR should have a non-controlling logic value to propagate an error due to an open defect to the cell output. This reasoning can be extended to non-basic cells as well. For example, for the AO22 cell (that has been mapped to basic gates) shown in Fig. 4,  $N4$  can be discarded as a logical neighbor of  $P3$  because it is one of the inputs of the AND cell and its value should be logic-1 to propagate the error through that cell. However, the other two side-inputs of cell  $R3$ ,  $N5$  and  $N6$ , remain as logical neighbors of  $P3$  because either one of them (or both) can be logic-0 to propagate the error through the OR cell to the cell output.

Thus, for the defective circuit shown in Fig. 4, the logical neighborhood of segment  $P3$  consists of  $N5$  and  $N6$ . On the other hand, DIAGNOSIX identifies nets  $N2, N3, N4, N5$  and  $N6$  along with the inputs of cell  $D$  as the logical neighbors.

In summary, the diagnosis procedure described in this work offers the following advantages when compared to DIAGNOSIX: (a) improved physical localization with individual segments instead of entire nets being reported by diagnosis, and (b) identification of nets and net segments that are more relevant to a particular defect.

#### IV. EXPERIMENTS

A defect-injection and simulation experiment using one of the functional blocks of the OpenSPARC T2 processor [28] (i.e., the non-cacheable unit (NCU)) is used to evaluate PADLOC. The following complex fault types are considered to model realistic defect behaviors.

- **Two-line bridge defects:** The biased voting model [27] is adopted to model bridge defects. Voltage of the bridged nets can be interpreted as either a logic-1 or logic-0 based on

the switching threshold of the receiver cell inputs. Potential bridge net pairs are extracted from the design layout. Note that the behaviors captured by the bridge fault models such as dominant, wired-AND, and wired-OR are a subset of this model and hence are not considered separately.

- **Open defects:** As discussed in Section III, the voltage at the floating net depends on several factors. This voltage can be interpreted as either a logic-1 or logic-0 based on the switching threshold of the receiver cell inputs. Open defect locations are extracted from the layout using the methodology described in Section III. To model the arbitrary behavior of an open defect, each receiver cell input corresponding to each identified location is randomly chosen to be faulty for a random subset of sensitizing test patterns.

- **Cell defects:** Open, bridge, and transistor defects (with varying resistance values) are injected into the layout of each cell. Each defective cell is simulated at transistor level to capture the cell-level defect behavior, which is then simulated to obtain a “tester response”.

Note that multiple nets (interconnects or intra-cell nets) can be faulty simultaneously for a test pattern in these fault models.

Each defect behavior is modeled using fault tuples [29]. 2,000 random instances of each fault type are injected in the NCU circuit to create a population of 6,000 faulty circuits. A test set of size 519 that achieves 100% stuck-at fault efficiency is generated using a commercial ATPG tool. Each faulty circuit is simulated at the logic level using FATSIM [30] to produce a tester response.

Fig. 5 shows an overview of the diagnosis flow. Path tracing [31] is first employed for each failed circuit to identify an initial set of candidates. Fault simulation is then performed by assuming an unknown value [32] at these candidate locations. The resulting simulation responses

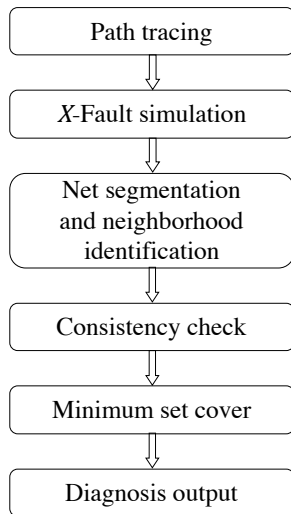


Fig. 5. Flow diagram showing the major steps of PADLOC.

are compared with the defective circuit response to find candidates that are compatible with the observations. Next, the methodology described in Section III is used to identify net segments (and their neighborhood) for each candidate. Then, the consistency check described in Section II is performed to eliminate candidate segments conservatively based on their neighborhood states. Minimum set covers are selected from the consistent candidate segments, where candidates in each cover jointly produce a response matching the observed circuit response. Finally, a custom fault model is derived from the set covers that precisely captures the functional impact of the defect on the circuit behavior.

Table 3 compares the diagnostic accuracy achieved for each fault type by DIAGNOSIX and PADLOC. Here, a defect is said to be accurately diagnosed (at the logic level) if the reported candidates include the net(s) or the cell used for defect injection. (Note that the accuracy and resolution of DIAGNOSIX and PADLOC cannot be compared directly at the physical level due to the improved layout granularity of PADLOC.)

TABLE 3  
DIAGNOSTIC ACCURACY COMPARISON FOR DIFFERENT DEFECT TYPES.

Defect type	DIAGNOSIX		PADLOC	
	Accurate	Inaccurate	Accurate	Inaccurate
Bridge	1892 (94.3%)	108	1936 (96.8%)	64
Open	1826 (91.3%)	174	1898 (94.9%)	102
Cell	2000 (100.0%)	0	2000 (100.0%)	0

PADLOC achieves an accuracy of 96.8% for bridge, 94.9% for open and 100.0% for cell defects. The average accuracy achieved is 97.2%, where the average improvement over DIAGNOSIX is 2.0% (2.3% and 3.9% for open and bridge defects, respectively). The accuracy improvement is believed to be resulting from two factors. First, neighbors that are more likely to correspond to the actual defect location are identified. Second, an entire net may be deemed inconsistent by DIAGNOSIX, but some of the segments may show consistency. The inclusion of these consistent segments in the diagnosis report results in an improvement in accuracy.

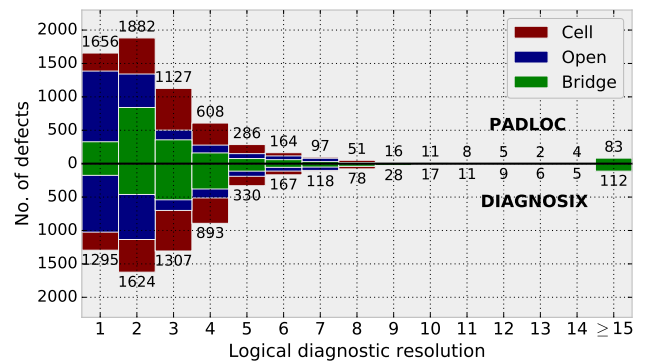


Fig. 6. Distribution of logical candidates for PADLOC and DIAGNOSIX.



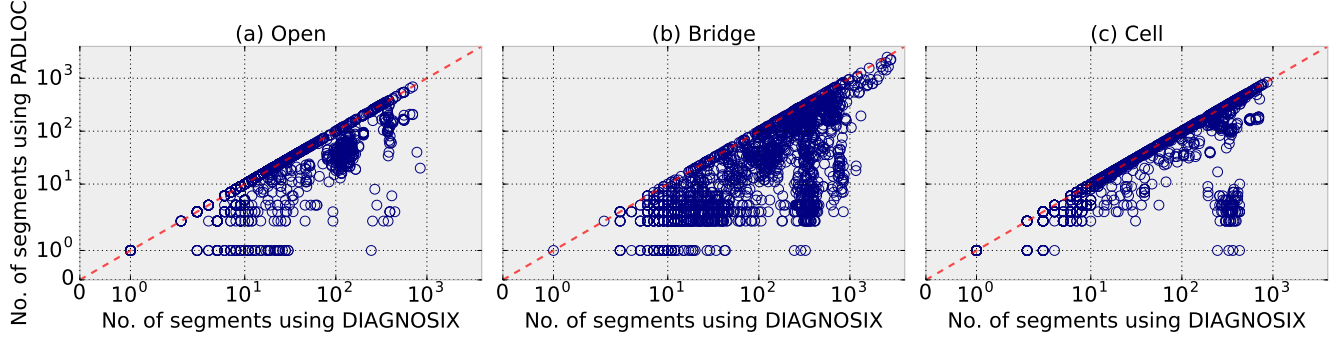


Fig. 7. Comparison of physical resolution (quantified as the number of segments) achieved by both approaches for (a) open, (b) bridge, and (c) cell defects.

Fig. 6 is a histogram of the diagnostic resolution (logical) for PADLOC (top half of the figure) and DIAGNOSIX (bottom half). Each bar is partitioned based on the defect type. Here, resolution is defined as the number of candidates, where a candidate can either be a cell or a logical signal. The average number of logical candidates reported by PADLOC is 1.1 for open, 3.9 for bridge, 2.9 for cell defects and 2.6 overall, whereas the average resolution is 3.1 for DIAGNOSIX. Further analysis shows that PADLOC improves resolution for 24.8% of defects while keeping resolution at the same level for the remaining defects.

In addition, PADLOC achieves perfect resolution for 1656 (27.6%) defects, an improvement of 27.9% over DIAGNOSIX. Specifically, 52.9% of open, 16.4% of bridge, and 13.5% of cell defects achieve a resolution of one, where the improvement over DIAGNOSIX for open and bridge defects is 24.5% and 87.4%, respectively. A low percentage of cell defects achieving perfect resolution can be attributed to the observation that all or a subset of inputs and outputs of a cell are included along with the cell itself in the candidate list. From further analysis, it is observed however, that only one cell candidate exists among all the candidates for 81.7% of the cell defects.

Moreover, a majority of the defects (92.6%) attain a resolution of at most five when PADLOC is applied. (A resolution of five or less is typically the resolution threshold required for PFA.) Also, 4.1% of defects have a resolution of greater than or equal to 15 with PADLOC, a reduction of 25.9% when compared to DIAGNOSIX.

To highlight the improvement in physical resolution, Fig. 7 compares the number of net segments reported by both approaches. The horizontal axis represents the resolution (i.e., the number of segments) for DIAGNOSIX, while the vertical axis represents the resolution for PADLOC. Each point on the plot corresponds to a particular diagnosis outcome. Points on the red dashed line indicate that both approaches report the same number of segments.

Fig. 7 shows that PADLOC has an average physical resolution of 76.5 segments while DIAGNOSIX has an

average of 138.7, which means that PADLOC reduces the number of segments by 44.8%. In addition, PADLOC returns 33.9 fewer segments per defect, with 60.4 fewer segments for bridge defects. Fig. 7 also reveals that the physical resolution is enhanced for 34.2% of open defects, 93.2% of bridge defects and 55.7% of cell defects. Moreover, PADLOC achieves perfect physical resolution for 212 defects, which is greater than 4X the number of defects reported by DIAGNOSIX with perfect resolution.

## V. CONCLUSIONS

This work presents a comprehensive physically-aware methodology for defect diagnosis we call PADLOC (Physically-Aware Defect Localization and Characterization). PADLOC consists of identifying defect locations and deriving its behavior based on the surrounding circuitry, instead of correlating the observed circuit response with fault models. In addition, PADLOC achieves improved physical localization compared to DIAGNOSIX by identifying the net segments more relevant to a particular defect.

Results from simulation experiments for over 6,000 defects reveal that PADLOC achieves an accuracy of 97.2%, with 27.6% of defects achieving perfect resolution and 92.6% of defects having a resolution of five or less. Additionally, PADLOC has an average physical resolution (quantified as the number of net segments) of 76.5 segments, a reduction of 44.8% when compared to DIAGNOSIX. Also, the physical resolution is improved for 61.3% of defects, on average. Dedicated test patterns can be generated to further improve the resolution. Current work extends PADLOC so that multiple defects and sequence-dependent defects (e.g. resistive opens) are also handled.

## REFERENCES

- [1] B. Benware, C. Schuermyer, M. Sharma, and T. Herrmann, "Determining a Failure Root Cause Distribution From a Population of Layout-Aware Scan Diagnosis Results," *IEEE Design Test of Computers*, vol. 29, no. 1, pp. 8–18, Feb 2012.
- [2] J. E. Nelson, T. Zanon, J. G. Brown, O. Poku, R. D. Blanton, W. Maly, B. Benware, and C. Schuermyer, "Extracting Defect Density and Size Distributions from Product ICs," *IEEE*

*Design Test of Computers*, vol. 23, no. 5, pp. 390–400, May 2006.

- [3] X. Yu and R. D. Blanton, “Estimating Defect-Type Distributions through Volume Diagnosis and Defect Behavior Attribution,” in *2010 IEEE International Test Conference*, Nov 2010, pp. 1–10.
- [4] Y. T. Lin and R. D. Blanton, “METER: Measuring Test Effectiveness Regionally,” *IEEE Transactions on Computer-Aided Design of Integrated Circuits and Systems*, vol. 30, no. 7, pp. 1058–1071, July 2011.
- [5] C. Xue and R. D. Blanton, “Predicting IC Defect Level Using Diagnosis,” in *IEEE 23rd Asian Test Symposium*, Nov 2014, pp. 113–118.
- [6] S. Holst and H. J. Wunderlich, “Adaptive Debug and Diagnosis without Fault Dictionaries,” in *12th IEEE European Test Symposium*, May 2007, pp. 7–12.
- [7] T. Bartenstein, D. Heaberlin, L. Huisman, and D. Sliwinski, “Diagnosing Combinational Logic Designs using the Single Location at-a-time (SLAT) Paradigm,” in *Proceedings International Test Conference 2001*, 2001, pp. 287–296.
- [8] J. A. Waicukauski and E. Lindbloom, “Failure Diagnosis of Structured VLSI,” *IEEE Design & Test of Computers*, vol. 6, no. 4, pp. 49–60, 1989.
- [9] S. Venkataraman and S. B. Drummonds, “POIROT: A Logic Fault Diagnosis Tool and its Applications,” in *Proceedings International Test Conference 2000*. IEEE, 2000, pp. 253–262.
- [10] J. C. M. Li and E. J. McCluskey, “Diagnosis of Sequence-dependent Chips,” in *Proceedings 20th IEEE VLSI Test Symposium*, 2002, pp. 187–192.
- [11] S.-Y. Huang, “Diagnosis of Byzantine Open-segment Faults [Scan Testing],” in *Test Symposium, 2002. (ATS '02). Proceedings of the 11th Asian*, Nov 2002, pp. 248–253.
- [12] Y. Sato, L. Yamazaki, H. Yamanaka, T. Ikeda, and M. Takakura, “A Persistent Diagnostic Technique for Unstable Defects,” in *Proceedings. International Test Conference*, 2002, pp. 242–249.
- [13] W. Zou, W. T. Cheng, and S. M. Reddy, “Interconnect Open Defect Diagnosis with Physical Information,” in *2006 15th Asian Test Symposium*, Nov 2006, pp. 203–209.
- [14] D. Arumi, R. Rodriguez-Montanes, J. Figueras, S. Eichenberger, C. Hora, and B. Kruseman, “Diagnosis of Interconnect Full Open Defects in the Presence of Fan-Out,” *IEEE Transactions on Computer-Aided Design of Integrated Circuits and Systems*, vol. 30, no. 12, pp. 1911–1922, 2011.
- [15] C. Liu, W. Zou, S. M. Reddy, W.-T. Cheng, M. Sharma, and H. Tang, “Interconnect Open Defect Diagnosis with Minimal Physical Information,” in *2007 IEEE International Test Conference*, Oct 2007, pp. 1–10.
- [16] K. Yamazaki, T. Tsutsumi, H. Takahashi, Y. Higami, T. Aikyo, Y. Takamatsu, H. Yotsuyanagi, and M. Hashizume, “A Novel Approach for Improving the Quality of Open Fault Diagnosis,” in *2009 22nd International Conference on VLSI Design*, Jan 2009, pp. 85–90.
- [17] W. Zou, W.-T. Cheng, and S. M. Reddy, “Bridge Defect Diagnosis with Physical Information,” in *14th Asian Test Symposium (ATS'05)*, Dec 2005, pp. 248–253.
- [18] M. Keim, N. Tamarapalli, H. Tang, M. Sharma, J. Rajski, C. Schuermyer, and B. Benware, “A Rapid Yield Learning Flow Based on Production Integrated Layout-Aware Diagnosis,” in *2006 IEEE International Test Conference*, Oct 2006, pp. 1–10.
- [19] M. Sharma, B. Benware, L. Ling, D. Abercrombie, L. Lee, M. Keim, H. Tang, W. T. Cheng, T. P. Tai, Y. J. Chang, R. Lin, and A. Man, “Efficiently Performing Yield Enhancements by Identifying Dominant Physical Root Cause from Test Fail Data,” in *2008 IEEE International Test Conference*, Oct 2008, pp. 1–9.
- [20] Y.-J. Chang, M.-T. Pang, M. Brennan, A. Man, M. Keim, G. Eide, B. Benware, and T.-P. Tai, “Experiences with Layout-aware Diagnosis - A Case Study,” in *Electronic Device Failure Analysis*, vol. 12, no. 12, 2010, pp. 12–18.
- [21] M. Sharma, S. Schwarz, J. Schmerberg, K. Yang, T.-P. Tai, Y.-S. Chen, C.-Y. Chuang, and F.-M. Kuo, “Layout-aware Diagnosis Leads to Efficient and Effective Physical Failure Analysis,” in *ISTFA 2011: Conference Proceedings of the 37th International Symposium for Testing and Failure Analysis*, 2011, pp. 87–90.
- [22] R. Desineni, O. Poku, and R. D. Blanton, “A Logic Diagnosis Methodology for Improved Localization and Extraction of Accurate Defect Behavior,” in *IEEE International Test Conference*, Oct 2006, pp. 1–10.
- [23] R. D. Blanton, W. C. Tam, X. Yu, J. E. Nelson, and O. Poku, “Yield Learning Through Physically Aware Diagnosis of IC-failure Populations,” *IEEE Design Test of Computers*, vol. 29, no. 1, pp. 36–47, Feb 2012.
- [24] W. C. Tam, O. Poku, and R. D. Blanton, “Precise Failure Localization using Automated Layout Analysis of Diagnosis Candidates,” in *45th ACM/IEEE Design Automation Conference*, June 2008, pp. 367–372.
- [25] Y. Xue, X. Li, and R. D. Blanton, “Improving Diagnostic Resolution of Failing ICs through Learning,” *IEEE Transactions on Computer-Aided Design of Integrated Circuits and Systems*, vol. PP, no. 99, 2016.
- [26] J. A. Porche and R. D. S. Blanton, “Physically-aware Diagnostic Resolution,” in *2014 IEEE 23rd Asian Test Symposium*, Nov 2014, pp. 206–211.
- [27] P. C. Maxwell and R. C. Aitken, “Biased Voting: A Method for Simulating CMOS Bridging Faults in the Presence of Variable Gate Logic Thresholds,” in *Proceedings of IEEE International Test Conference - (ITC)*, Oct 1993, pp. 63–72.
- [28] I. Parulkar, A. Wood, J. C. Hoe, B. Falsafi, S. V. Adve, J. Torrellas, and S. Mitra, “OpenSPARC: An open platform for hardware reliability experimentation,” in *Fourth Workshop on Silicon Errors in Logic-System Effects (SELSE)*. Citeseer, 2008.
- [29] R. D. Blanton, K. N. Dwarakanath, and R. Desineni, “Defect Modeling Using Fault Tuples,” *IEEE Transactions on Computer-Aided Design of Integrated Circuits and Systems*, vol. 25, no. 11, pp. 2450–2464, Nov 2006.
- [30] K. N. Dwarakanath and R. D. Blanton, “Universal Fault Simulation Using Fault Tuples,” in *Proceedings of the 37th Annual Design Automation Conference*. ACM, 2000, pp. 786–789.
- [31] S. Venkataraman and W. K. Fuchs, “A Deductive Technique for Diagnosis of Bridging Faults,” in *1997 Proceedings of IEEE International Conference on Computer Aided Design (ICCAD)*, Nov 1997, pp. 562–567.
- [32] V. Boppana and M. Fujita, “Modeling the Unknown! Towards Model-independent Fault and Error Diagnosis,” in *Proceedings International Test Conference 1998*, Oct 1998, pp. 1094–1101.